

***Supporting Information***

**A new type of double-chain based 3D lanthanide(III) metal–organic framework demonstrating proton conduction and tunable emission**

Min Zhu,<sup>a,b</sup> Zhao-Min Hao,<sup>a,b</sup> Xue-Zhi Song,<sup>a,b</sup> Xing Meng,<sup>a,b</sup> Shu-Na Zhao,<sup>a,b</sup> Shu-Yan Song,<sup>a</sup> Hong-Jie Zhang <sup>\*a</sup>

<sup>a</sup>State Key Laboratory of Rare Earth Resource Utilization, Changchun Institute of Applied Chemistry, Chinese Academy of Sciences, 5625 Renmin Street, Changchun 130022, China

Tel: +86-431-85262127; Fax: +86-431-85698041; E-mail: [hongjie@ciac.ac.cn](mailto:hongjie@ciac.ac.cn)

<sup>b</sup>University of Chinese Academy of Sciences, Beijing, 100049, China

\*Corresponding author

Email: [hongjie@ciac.ac.cn](mailto:hongjie@ciac.ac.cn) (Hong-Jie Zhang)

Tel: 86-431-85262127.

Fax: 86-431-85698041.

## 1. Experimental Section

All commercially available chemical materials were of analytical grade and were used as received without further purification. The ligand **L**, (*N*-phenyl-*N'*-phenyl bicyclo[2.2.2]oct-7-ene-2,3,5,6-tetracarboxdiimide tetracarboxylic acid) was synthesized according to the previous report.<sup>1</sup>

### Synthesis of **[EuL(H<sub>2</sub>O)<sub>3</sub>]·2H<sub>2</sub>O**.

A mixture of Eu(NO<sub>3</sub>)<sub>3</sub>·6H<sub>2</sub>O (0.05 mmol), **L** (0.05 mmol), ethanol (3.0 mL) and H<sub>2</sub>O (3.0 mL) was added to a 15 mL Teflon-lined stainless-steel autoclave and heated at 80°C for 72 h. After it was cooled to room temperature, colorless block crystals suitable for X-ray diffraction analysis were collected, washed with ethanol and dried under ambient conditions with a yield of 74% based on **L**. Elemental analysis for C<sub>28</sub>H<sub>25</sub>N<sub>2</sub>O<sub>17</sub>Eu (813.47) (%): calcd. C 41.34, H 3.10, N 3.44; found C 41.36, H 3.05, N 3.49. Other **LnL** complexes were synthesized similar to **EuL** using compounds Ln(NO<sub>3</sub>)<sub>3</sub>·6H<sub>2</sub>O.

### Synthesis of Ln-doped analogs.

#### i. Synthesis of **Eu<sub>x</sub>Tb<sub>1-x</sub>L**

Typically, a mixture of Eu(NO<sub>3</sub>)<sub>3</sub>·6H<sub>2</sub>O aqueous solution (0.04 mol/L, *a* mL), Tb(NO<sub>3</sub>)<sub>3</sub>·6H<sub>2</sub>O aqueous solution (0.08 mol/L, *b* mL), **L** (0.05 mmol), ethanol (3.0 mL) and H<sub>2</sub>O (3.0-*a*-*b* mL), was added to a 15 mL Teflon-lined stainless-steel autoclave and heated at 80°C for 72 h. After it was cooled to room temperature, colorless crystalline-like powder were collected, washed with ethanol and dried under ambient conditions.

#### ii. Synthesis of **Dy<sub>x</sub>Eu<sub>y</sub>Gd<sub>1-x-y</sub>L** and **Sm<sub>x</sub>Eu<sub>y</sub>Gd<sub>1-x-y</sub>L**

The procedure was similar to the above. For **Dy<sub>x</sub>Eu<sub>y</sub>Gd<sub>1-x-y</sub>L**, a mixture of Dy(NO<sub>3</sub>)<sub>3</sub>·6H<sub>2</sub>O aqueous solution (0.04 mol/L, *a* mL), Eu(NO<sub>3</sub>)<sub>3</sub>·6H<sub>2</sub>O aqueous solution (1.25×10<sup>-3</sup> mol/L, *b* mL), Gd(NO<sub>3</sub>)<sub>3</sub>·6H<sub>2</sub>O aqueous solution (0.08 mol/L, *c* mL), **L** (0.05 mmol), ethanol (3.0 mL) and H<sub>2</sub>O (3.0-*a*-*b*-*c* mL) was added. For **Sm<sub>x</sub>Eu<sub>y</sub>Gd<sub>1-x-y</sub>L**, a mixture of Sm(NO<sub>3</sub>)<sub>3</sub>·6H<sub>2</sub>O aqueous solution (0.04 mol/L, *a* mL), Eu(NO<sub>3</sub>)<sub>3</sub>·6H<sub>2</sub>O aqueous solution (0.04 mol/L, *b* mL), Gd(NO<sub>3</sub>)<sub>3</sub>·6H<sub>2</sub>O aqueous solution (0.08 mol/L, *c* mL), **L** (0.05 mmol), ethanol (3.0 mL) and H<sub>2</sub>O (3.0-*a*-*b*-*c* mL)

was added (The volume  $a$ ,  $b$ ,  $c$  of  $\text{Ln}(\text{NO}_3)_3 \cdot 6\text{H}_2\text{O}$  aqueous solution was calculated from the corresponding doping concentration  $x$ ,  $y$ ). The colorless crystalline-like powder of products were collected, washed with ethanol and dried under ambient conditions. The PXRD patterns of all the doped complexes are characterized, and convince the purity and the intact structure of them (Fig. S2).

### General Methods

Elemental analyses (C, H, and N) were performed on a Perkin-Elmer 2400 CHN Elemental Analyzer. The TG analyses was performed on a Perkin–Elmer Thermal Analysis Pyris Diamond TG/DTA instrument in air atmosphere with a heating rate of 10 °C/min. The PXRD patterns were obtained with a Bruker D8-ADVANCE diffractometer equipped with Cu K $\alpha$ 1 ( $\lambda = 1.5406 \text{ \AA}$ ; 1600 W, 40 kV, 40 mA), and the scanning rate is 5°/min,  $2\theta$  ranging from 5–40°. The simulated PXRD patterns were calculated by using single-crystal X-ray diffraction data and processed by the free *Mercury v1.4* program provided by the Cambridge Crystallographic Data Center.

### X-ray crystallography

The X-ray intensity data for **EuL** were collected on a Bruker SMART APEX-II CCD diffractometer with graphite monochromatized Mo-K $\alpha$  radiation ( $\lambda = 0.71073 \text{ \AA}$ ) operating at 1.5 kW (50 kV, 30 mA) at room temperature. Data integration and reduction were processed with SAINT software.<sup>2</sup> Multiscan absorption corrections were applied with the SADABS program.<sup>3</sup> The structure was solved by direct methods and refined employing full-matrix least squares techniques based on  $F^2$  using the SHELXTL-97 crystallographic software package.<sup>4</sup> All non-hydrogen atoms were refined with anisotropic temperature parameters except the free solvent molecules. All hydrogen atoms attached to carbon atoms were generated geometrically and refined using a riding model. The detailed crystallographic data and structure refinement parameters for these compounds are summarized in Table S1. Crystallographic data for the structure reported in this paper have been deposited in the Cambridge Crystallographic Data Center with CCDC Number: 971185 for **EuL**.

## References

- 1 Z. J. Zhang, W. Shi, Z. Niu, H. H. Li, B. Zhao, P. Cheng, D. Z. Liao and S. P. Yan, *Chem. Commun.*, 2011, **47**, 6425.
- 2 SAINT, *Program for Data Extraction and Reduction*, Bruker AXS, Inc., Madison, WI, 2001.
- 3 G. M. Sheldrick, *SADABS*, University of Göttingen, Göttingen, Germany 1996.
- 4 (a) G. M. Sheldrick, *SHELXS 97, Program for the Solution of Crystal Structure*, University of Göttingen, Göttingen, Germany 1997; (b) G. M. Sheldrick, *SHELXS 97, Program for the Crystal Structure Refinement*, University of Göttingen, Göttingen, Germany 1997.

## 2. Crystal data for LnL

**Table S1.** Crystal and Structure Refinement Data for **EuL**.

Compound	<b>EuL</b>
Empirical formula	C <sub>28</sub> H <sub>25</sub> N <sub>2</sub> O <sub>17</sub> Eu
Formula weight	813.47
T, K	296(2)
Crystal system	Monoclinic
Space group	P2 <sub>1</sub> /n
a/Å	15.535(4)
b/Å	12.555(3)
c/Å	15.636(4)
α/deg	90.00
β/deg	104.005(5)
γ/deg	90.00
V/Å <sup>3</sup>	2959.0(13)
Z	4
D <sub>calc</sub> /g cm <sup>-3</sup>	1.801
μ/mm <sup>-1</sup>	2.206
F(000)	1580
Reflections collected	18291
Independnt reflectins	5935 ( <i>R</i> <sub>int</sub> = 0.0275)
<i>R</i> <sub>1</sub> <sup>a</sup> , <i>wR</i> <sub>2</sub> <sup>b</sup> [I > 2σ(I)]	0.0296, 0.0822
<i>R</i> <sub>1</sub> <sup>a</sup> , <i>wR</i> <sub>2</sub> <sup>b</sup> (all data)	0.0363, 0.0860
Goodness on <i>F</i> <sup>2</sup>	1.032

**Table S2.** Selected bond lengths ( $\text{\AA}$ ) and angles ( $^\circ$ ) for **EuL**.

<b>EuL</b>			
Eu(1)-O(7)	2.287(3)	Eu(1)-O(5)	2.391(3)
Eu(1)-O(8)	2.415(3)	Eu(1)-OW4	2.431(3)
Eu(1)-OW5	2.456(3)	Eu(1)-OW3	2.472(3)
Eu(1)-O(12)	2.468(3)	Eu(1)-O(11)	2.556(3)
Eu(1)-O(10)	2.678(3)	O(7)-Eu(1)-O(5)	124.35(11)
O(8)-Eu(1)-O(7)	99.99(10)	O(5)-Eu(1)-O(8)	75.24(10)
O(7)-Eu(1)-OW4	151.80(12)	O(5)-Eu(1)-OW4	79.69(11)
O(8)-Eu(1)-OW4	69.89(11)	O(7)-Eu(1)-OW5	75.55(10)
O(5)-Eu(1)-OW5	76.87(10)	O(8)-Eu(1)-OW5	142.13(10)
OW4-Eu(1)-OW5	128.81(10)	O(7)-Eu(1)-O(12)	130.03(10)
O(5)-Eu(1)-O(12)	76.56(9)	O(8)-Eu(1)-O(12)	129.97(9)
OW4-Eu(1)-O(12)	64.97(10)	OW5-Eu(1)-O(12)	65.60(9)
O(7)-Eu(1)-OW3	73.89(12)	O(5)-Eu(1)-OW3	144.56(11)
O(8)-Eu(1)-OW3	71.42(11)	OW4-Eu(1)-OW3	77.92(12)
OW5-Eu(1)-OW3	138.34(11)	O(12)-Eu(1)-OW3	117.01(10)
O(7)-Eu(1)-O(11)	90.87(10)	O(5)-Eu(1)-O(11)	127.86(9)
O(8)-Eu(1)-O(11)	140.84(11)	OW4-Eu(1)-O(11)	82.85(11)

**Table S3.** The cell parameters of **LnL** complexes (Ln = Pr, Nd, Sm, Eu, Gd, Tb, Dy, Er, Tm, Yb, Y, Monoclinic,  $P2_1/n$ ,  $\alpha=\gamma=90^\circ$ ).

Ln	$a/\text{\AA}$	$b/\text{\AA}$	$c/\text{\AA}$	$\beta/^\circ$	$V/\text{\AA}^3$
Pr	15.56	12.65	15.82	104.08	3020
Nd	15.57	12.62	15.79	104.07	3007
Sm	15.45	12.52	15.57	103.82	2925
Eu	15.535(4)	12.555(3)	15.636(4)	104.005(5)	2959.0(13)
Gd	15.61	12.59	15.71	104.01	2995
Tb	15.57	12.54	15.67	103.87	2969
Dy	15.49	12.65	15.83	103.94	3012
Er	15.00	12.54	15.98	103.51	2923
Tm	15.09	12.72	16.44	103.09	3073
Yb	14.93	12.60	16.25	103.16	2975
Y	15.23	12.63	15.95	103.65	2982

### 3. XRD analyses and TG analysis

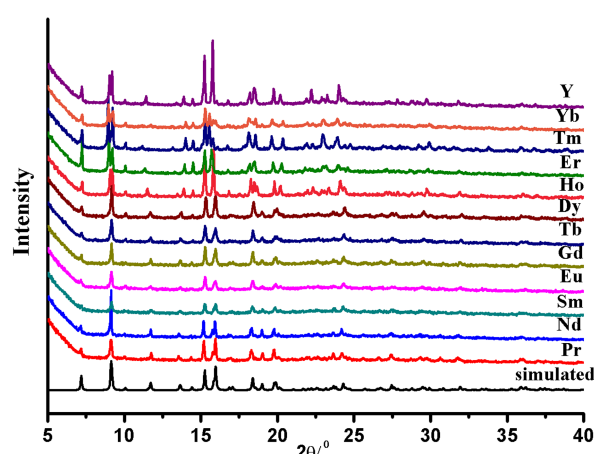


**Fig. S1** Powder XRD patterns of the whole  $\text{LnL}$  compounds (except La, Ce, Pm).

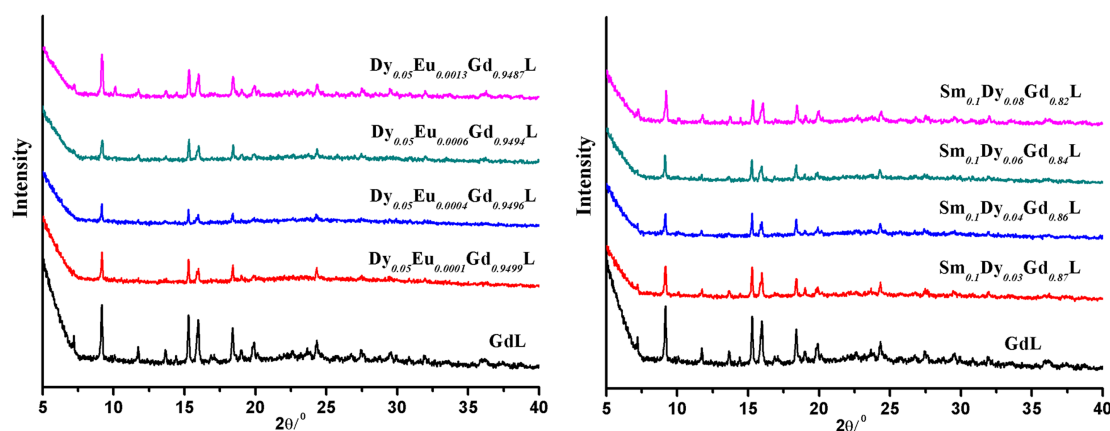


**Fig. S2** Powder XRD patterns of the  $\text{Dy}_x\text{Eu}_y\text{Gd}_{1-x-y}\text{L}$  and  $\text{Sm}_x\text{Dy}_y\text{Gd}_{1-x-y}\text{L}$  complexes.

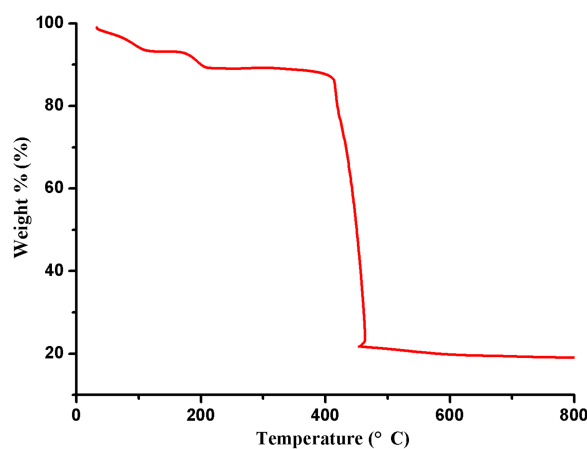
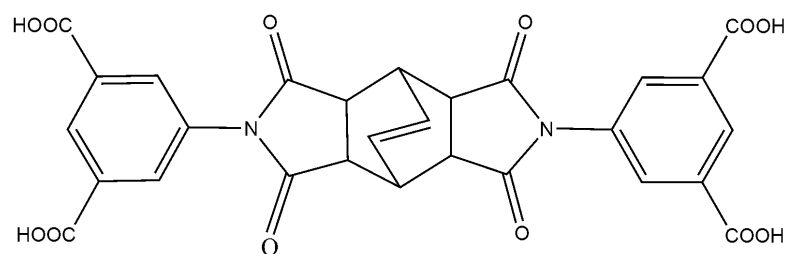


**Fig. S3** TG curve of  $\text{EuL}$  complex.

#### 4. Additional figures for structural information of EuL



**Scheme S1** The structure of ligand molecule.

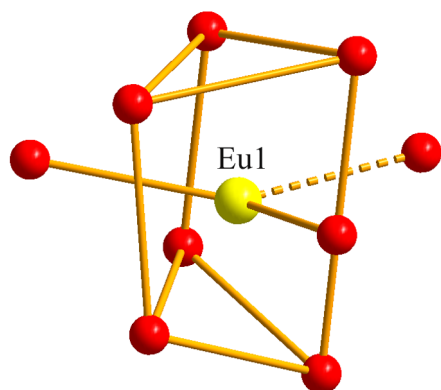


**Fig. S4** The coordination fashion of the Eu Center.

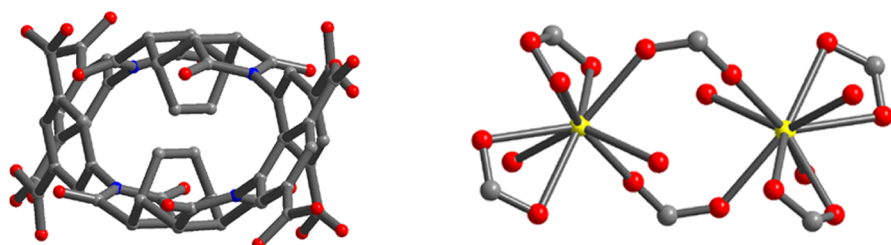


**Fig. S5** View of a pair of ligands with different conformation (left) and the binuclear Eu units (right).

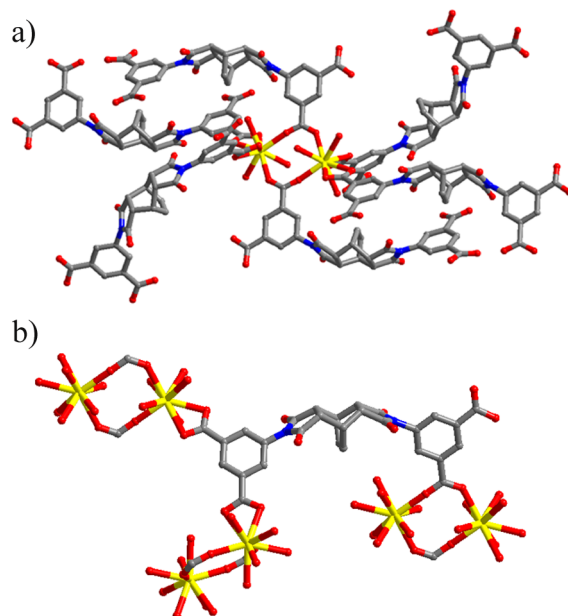


**Fig. S6** The coordination fashion of binuclear Eu unit (a) and ligand molecule (b).

## 5. Proton conductivity measurements

The powder for alternating-current (ac) impedance measurements was prepared by grinding the sample into a homogeneous powder with a mortar and pestle. The powders of **EuL** and **DyL** were then added to a standard 8 mm die, sandwiched between two stainless steel electrodes and pressed at 10 MPa for 3 min. The two pellets were both 8 mm in diameter and 0.8 mm in thickness. Measurements were carried out using an impedance and gain-phase analyzer (PARSTAT 4000, Ametek, USA) over a frequency range from 0.1 Hz to 1 MHz, with a quasi-four-probe electrochemical cell and an applied ac voltage of 100 mV. Measurements were taken in the temperature range of 25–75°C with 97% relative humidity (controlled by using an HDHWHS-50 incubator). ZSimpWin software was used to extrapolate impedance data results by means of an equivalent circuit simulation to complete the Nyquist plot and obtain the resistance values. Conductivity was calculated using the following equation:

$$\sigma = L / RS$$

Where  $L$  and  $S$  are the thickness (cm) and cross-sectional area ( $\text{cm}^2$ ) of the pellet respectively, and  $R$ , which was extracted directly from the impedance plots, is the bulk resistance of the sample and  $\sigma$  is the conductivity ( $\text{S cm}^{-1}$ ).

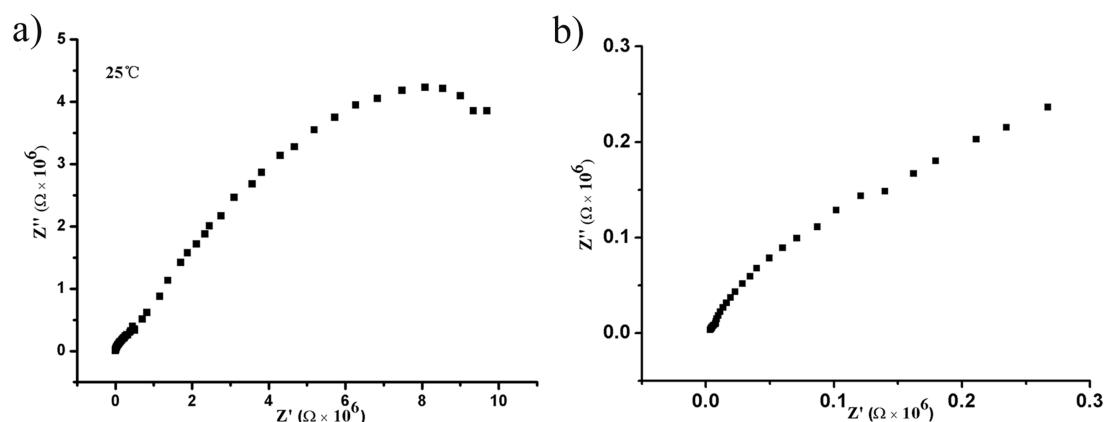


**Fig. S7** a) Nyquist plot of EuL at 25°C under 97% RH; b) view of the first depressed semicircle related to the bulk phase at high frequency at 25°C

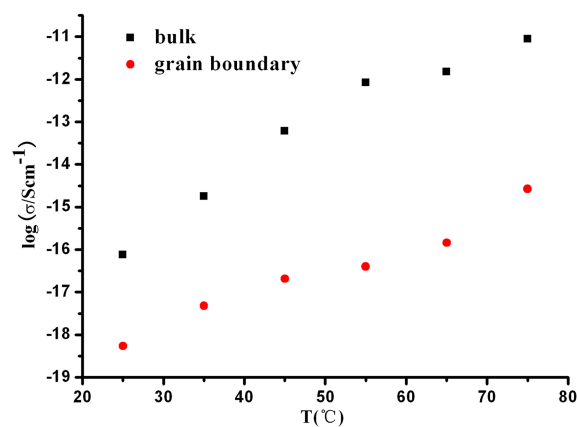


**Fig. S8**  $\log(\sigma/S \text{ cm}^{-1})$  (bulk and grain boundary) versus temperature plot of EuL from 25 to 75°C

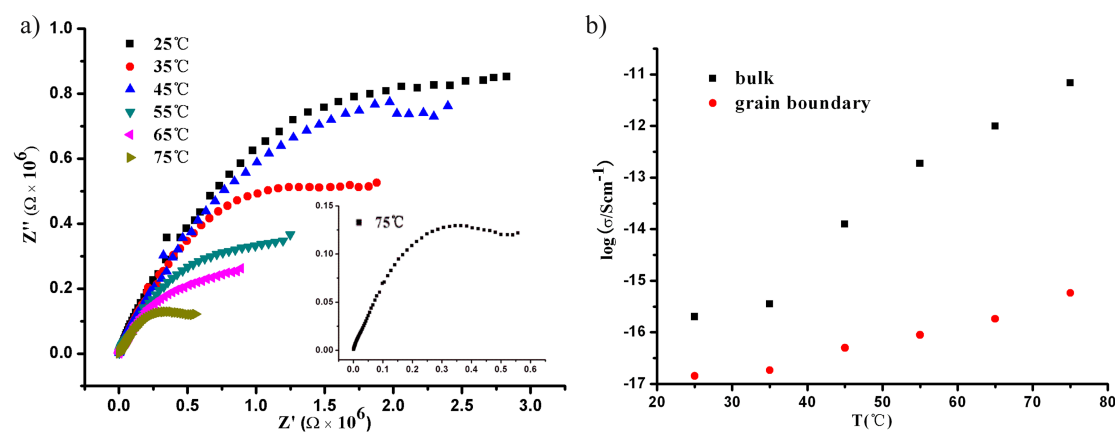


**Fig. S9** a) Nyquist plots of DyL from 25 to 75°C (insert: 75°C); b)  $\log(\sigma/S \text{ cm}^{-1})$  (bulk and grain boundary) versus temperature plot of DyL from 25 to 75°C

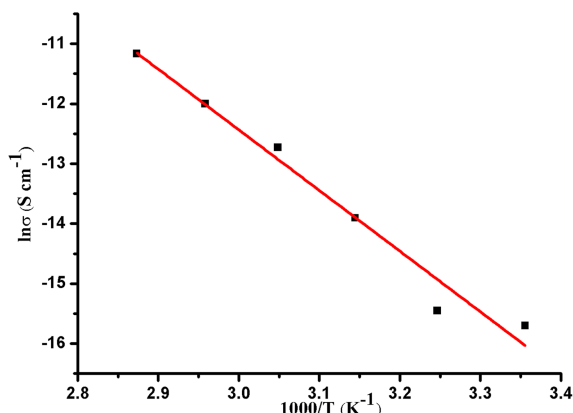


**Fig. S10** Temperature dependency of proton conductivity for the bulk phase of **DyL**.

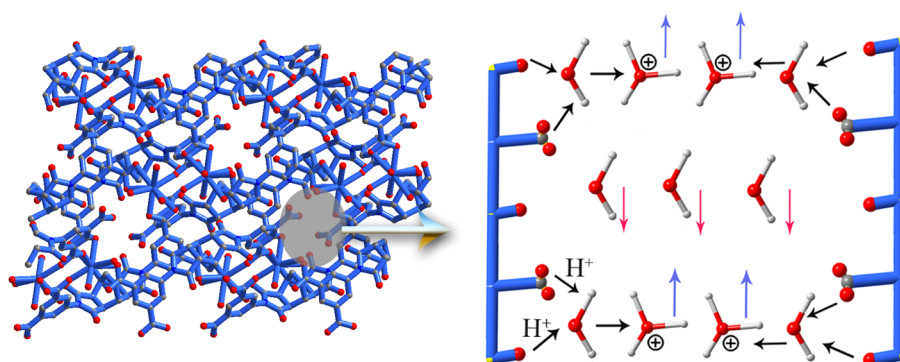


**Fig. S11** View of the possible proton transport via Vehicle Mechanism in the structure.

## 6. Luminescent measurements

The fluorescence excitation and emission spectra were recorded at room temperature with a Hitachi F-4500 spectrophotometer equipped with a 150 W Xenon lamp as an excitation source. The excitation wavelength is 293 nm by monitoring the characteristic emission (613 nm) of the  $Eu^{3+}$  ion. The photomultiplier tube (PMT) voltage was 700 V in all the measurements, except 400 V for Eu-Tb co-doped complexes. The scan speed was 1200 nm/min. The slit widths of excitation and emission were set the same in the measurements of each series of Ln-doped analogs. The luminescence decay curve was obtained from a Lecroy Wave Runner 6100

Digital Oscilloscope (1 GHz) using a tunable laser (pulse width = 4 ns, gate = 50 ns) as the excitation source (Continuum Sunlite OPO). The luminescence lifetime was calculated by Origin 8.0 software package. The quantum yield measurement was performed on a FLS920 from Edinburgh Instruments, and the excitation wavelength is 293 nm.

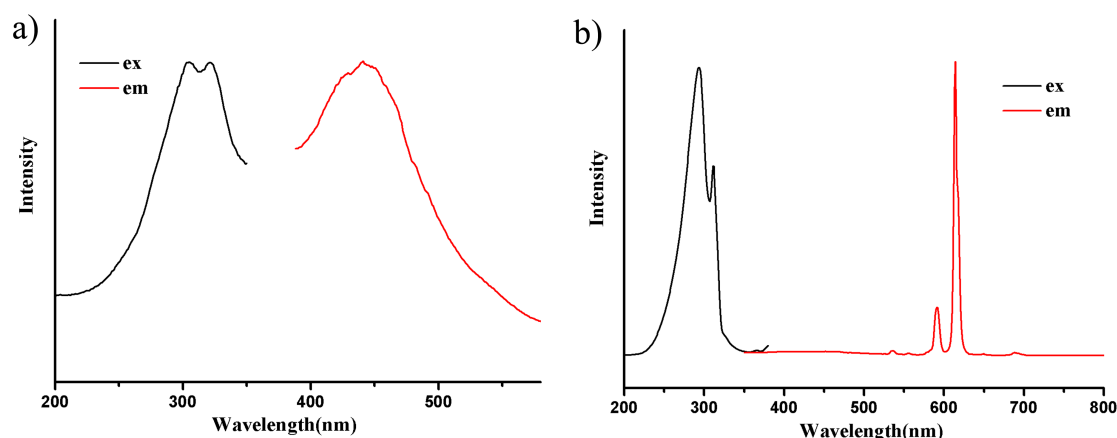


**Fig. S12** a) The exitation and emission spectra of ligand molecule ( $\lambda_{\text{ex}} = 305$  nm); b) the exitation and emission spectra of **EuL** ( $\lambda_{\text{ex}} = 293$  nm).

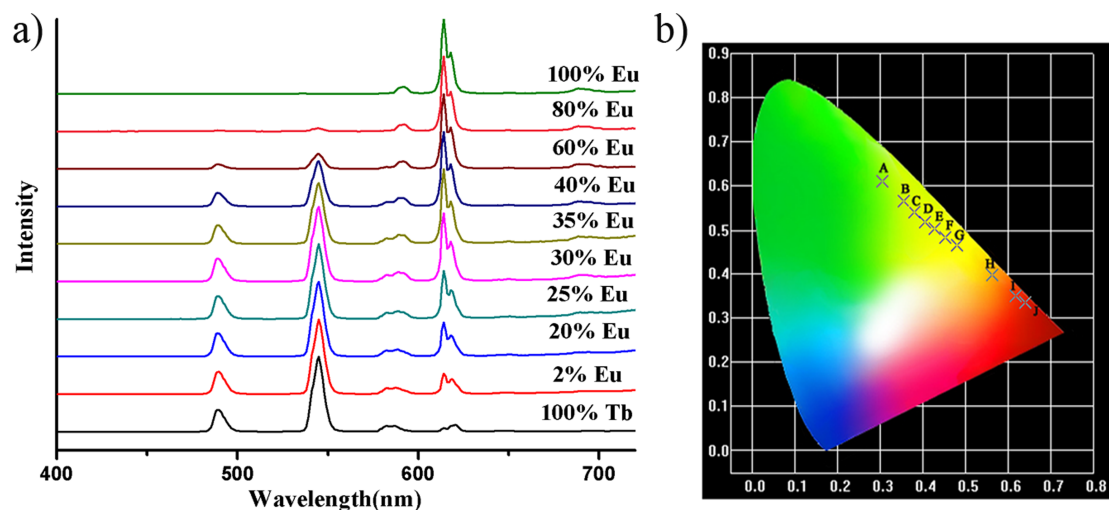


**Fig. S13** a) The emission spectra of the mixed MOF  $\text{Eu}_x\text{Tb}_{1-x}\text{L}$  ( $\lambda_{\text{ex}} = 293$  nm); b) CIE chromaticity diagram for  $\text{Eu}_x\text{Tb}_{1-x}\text{L}$  (A→J, increasing the concentration of Eu(III))

Under UV excitation at 293 nm, the **EuL** complex shows typical peaks at 591, 613, 650 and 691 nm, which are attributed to  $^5D_0 \rightarrow ^7F_J$  ( $J = 1-4$ ) transitions, with the  $^5D_0 \rightarrow ^7F_2$  (613 nm) red emission as the most prominent group; the **TbL** complex displays bonds at 489, 544, 582, 619 and 647 nm, corresponding to the  $^5D_4 \rightarrow ^7F_J$  ( $J = 6-2$ ) transitions of  $Tb^{3+}$  ion, with the  $^5D_4 \rightarrow ^7F_5$  (544 nm) green emission as the most prominent group. The ligand exhibits a broad emission band peaked at 436 nm which presumably attributed to  $n-\pi^*$  or  $\pi-\pi^*$  transitions when excited at 305 nm, while similar bond in the spectra of **Eu/TbL** couldn't be observed, indicating the efficient ligand-to-metal energy transfer.

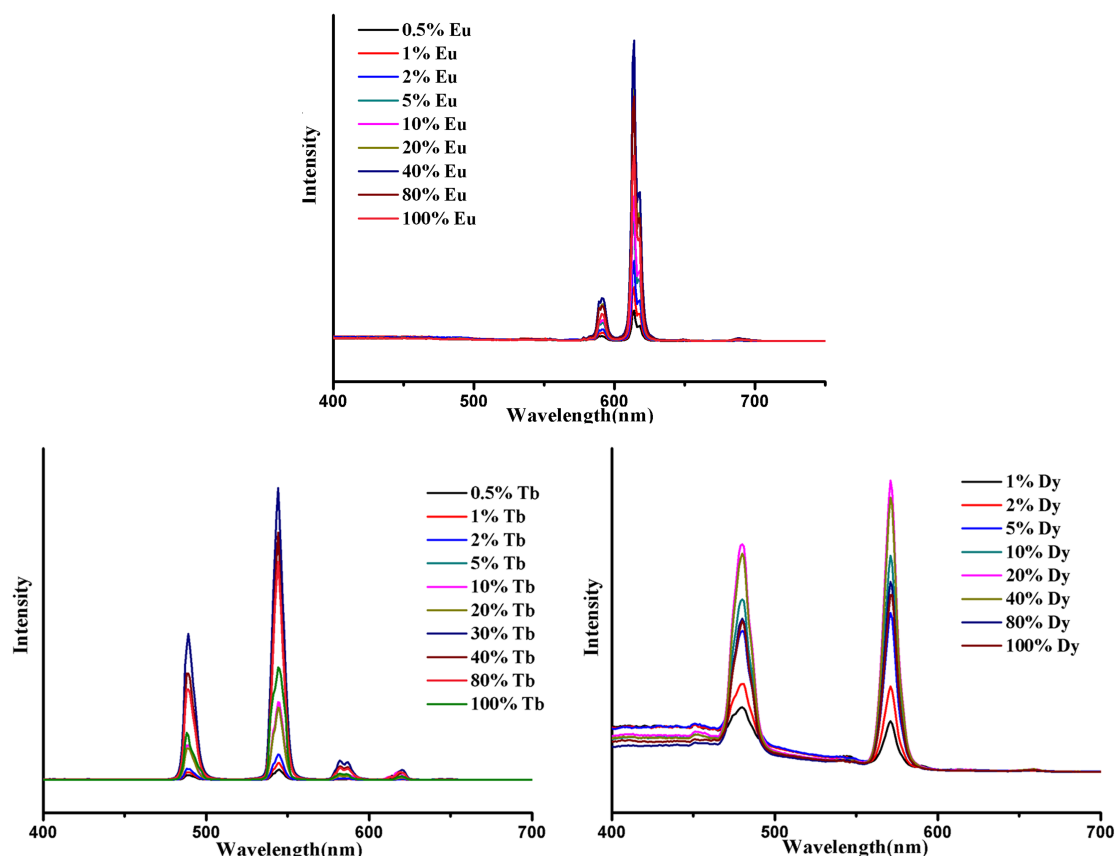


**Fig. S14** The emission spectra of  $Ln_xGd_{1-x}L$  ( $\lambda_{ex} = 293$  nm) ( $Ln = Eu, Tb, Dy$ ).

Once 40%  $Eu^{3+}$  was doped into Gd compounds ( $Eu_{0.4}Gd_{0.6}L$ ), the emission intensity of  $^5D_0 \rightarrow ^7F_2$  transition has increased by 1.6 times in contrast to **EuL**. When 30%  $Tb^{3+}$  was doped, the emission intensity of the peak at 544 nm ( $^5D_4 \rightarrow ^7F_5$ ) increased by 2.63 times. As for Dy-doped complex, it shows the characteristic transitions for the  $Dy^{3+}$  ion:  $^4F_{9/2} \rightarrow ^6H_{15/2}$  (480 nm) and  $^4F_{9/2} \rightarrow ^6H_{13/2}$  (571 nm)

transitions, and a weak broad band between 400 and 450 nm for ligand. The emission intensity of the peak at 571 nm increased by 1.65 times when 20% Dy<sup>3+</sup> was doped.

**Table S3.** The CIE coordinates of  $\text{Dy}_x\text{Eu}_y\text{Gd}_{1-x-y}\text{L}$ .

$\text{Dy}_x\text{Eu}_y\text{Gd}_{1-x-y}\text{L}$	CIE (X, Y)
$\text{Dy}_{0.05}\text{Eu}_{0.0001}\text{Gd}_{0.9499}\text{L}$	(0.302, 0.334)
$\text{Dy}_{0.05}\text{Eu}_{0.0004}\text{Gd}_{0.9496}\text{L}$	(0.323, 0.348)
$\text{Dy}_{0.05}\text{Eu}_{0.0006}\text{Gd}_{0.9494}\text{L}$	(0.338, 0.350)
$\text{Dy}_{0.05}\text{Eu}_{0.0013}\text{Gd}_{0.9487}\text{L}$	(0.348, 0.344)

**Table S4.** The CIE coordinates of  $\text{Sm}_x\text{Dy}_y\text{Gd}_{1-x-y}\text{L}$ .

$\text{Sm}_x\text{Dy}_y\text{Gd}_{1-x-y}\text{L}$	CIE (X, Y)
$\text{Sm}_{0.1}\text{Dy}_{0.03}\text{Gd}_{0.87}\text{L}$	(0.301, 0.304)
$\text{Sm}_{0.1}\text{Dy}_{0.04}\text{Gd}_{0.86}\text{L}$	(0.301, 0.309)
$\text{Sm}_{0.1}\text{Dy}_{0.06}\text{Gd}_{0.84}\text{L}$	(0.309, 0.329)
$\text{Sm}_{0.1}\text{Dy}_{0.08}\text{Gd}_{0.82}\text{L}$	(0.313, 0.337)

### Luminescence Decay measurements on the LnL and Ln<sup>3+</sup> doped materials

The luminescence decay curves were fit well with monoexponential decays using the following equation:

$$y = Ae(-x/t) + y_0$$

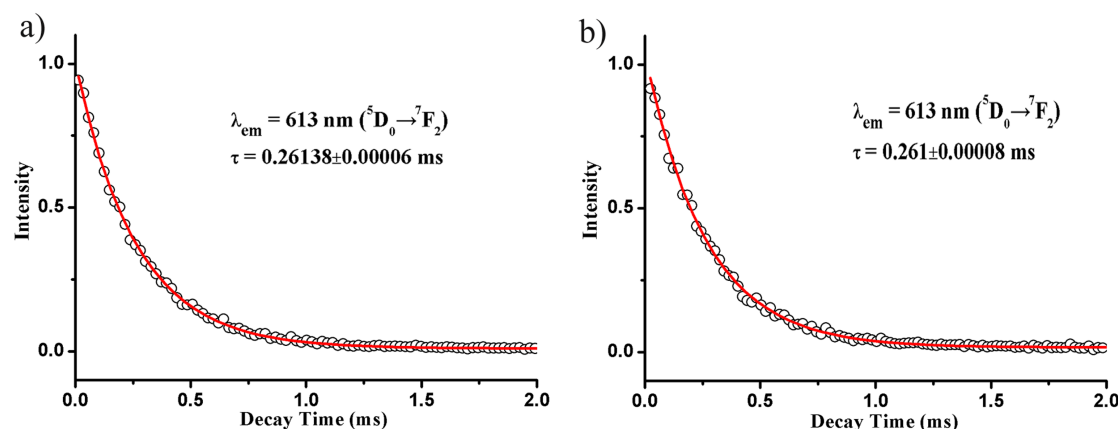


**Fig. S15** Luminescence decay curves for the  $^5\text{D}_0 \rightarrow ^7\text{F}_2$  (613 nm) emission of EuL and Eu<sub>0.3</sub>Gd<sub>0.7</sub>L.

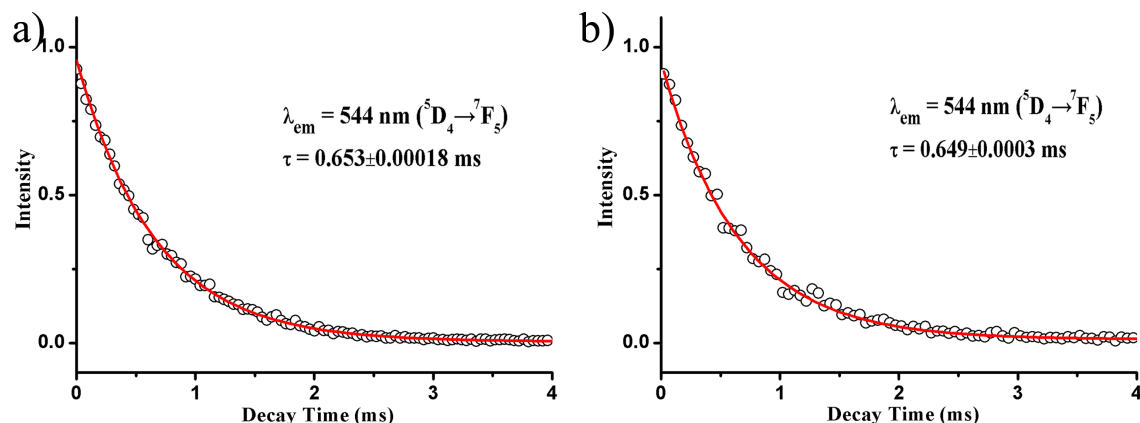


**Fig. S16** Luminescence decay curves for the  $^5\text{D}_4 \rightarrow ^7\text{F}_5$  (544 nm) emission of **TbL** and **Tb<sub>0.3</sub>Gd<sub>0.7</sub>L**.

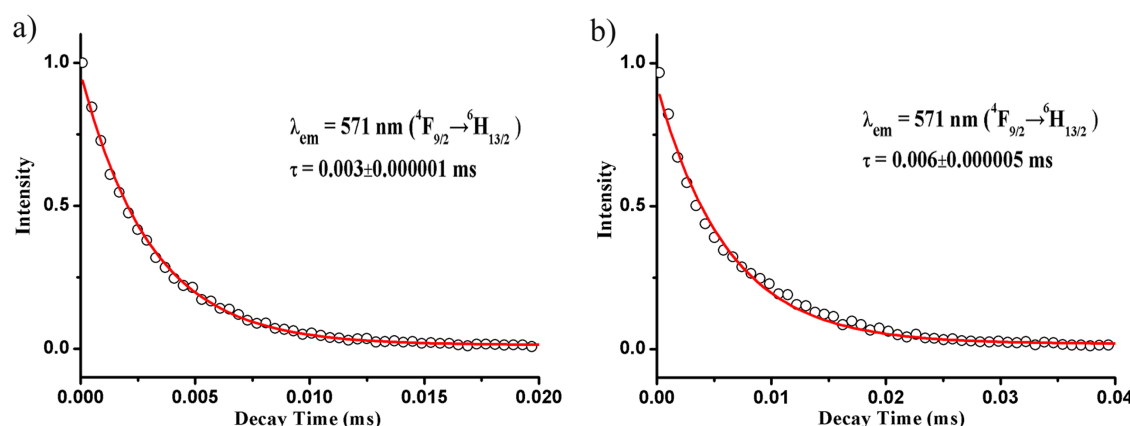


**Fig. S17** Luminescence decay curves for the  $^4\text{F}_{9/2} \rightarrow ^6\text{H}_{13/2}$  (571 nm) emission of **DyL** and **Dy<sub>0.2</sub>Gd<sub>0.8</sub>L**.

**Table S5.** Luminescence lifetime ( $\mu\text{s}$ ) and quantum yields (%) of  $\text{Ln}^{3+}$  ions in corresponding **LnL** and doped materials.

$\text{Ln}^{3+}$ ( <b>LnL</b> )	luminescence lifetime $\tau$ ( $\mu\text{s}$ )	quantum yields $\Phi$ (%)
$\text{Eu}^{3+}$ ( <b>EuL</b> )	261	12.9
$\text{Eu}^{3+}$ ( <b>Eu<sub>0.3</sub>Gd<sub>0.7</sub>L</b> )	261	11.8
$\text{Tb}^{3+}$ ( <b>TbL</b> )	653	42.2
$\text{Tb}^{3+}$ ( <b>Tb<sub>0.3</sub>Gd<sub>0.7</sub>L</b> )	649	35
$\text{Dy}^{3+}$ ( <b>DyL</b> )	3	0.1
$\text{Dy}^{3+}$ ( <b>Dy<sub>0.2</sub>Gd<sub>0.8</sub>L</b> )	6	0.2